BIOCHEMISTRY
including biophysical chemistry & molecular biology
Article

Biochemistry **2009,** *48,* 7473–7481 7473
DOI: 10.1021/bi900694p

Physical Interaction between Replication Protein A (RPA) and MRN: Involvement of RPA2 Phosphorylation and the N-Terminus of RPA1[†]

Greg G. Oakley,[‡] Kristin Tillison,[§] Stephen A. Opiyo,[‡] Jason G. Glanzer,[‡] Jeffrey M. Horn,[∥] and Steve M. Patrick*[,§]

[‡]*College of Dentistry, University of Nebraska Medical Center, Lincoln, Nebraska 68583,* [§]*Department of Biochemistry and Cancer Biology, University of Toledo Health Science Campus, Toledo, Ohio 43614, and* [∥]*Wright State University, Dayton, Ohio 45435*

Received April 22, 2009; Revised Manuscript Received July 7, 2009

ABSTRACT: Replication protein A (RPA) is a heterotrimeric protein consisting of RPA1, RPA2, and RPA3 subunits that binds to single-stranded DNA (ssDNA) with high affinity. The response to replication stress requires the recruitment of RPA and the MRE11−RAD50−NBS1 (MRN) complex. RPA bound to ssDNA stabilizes stalled replication forks by recruiting checkpoint proteins involved in fork stabilization. MRN can bind DNA structures encountered at stalled or collapsed replication forks, such as ssDNA−double-stranded DNA (dsDNA) junctions or breaks, and promote the restart of DNA replication. Here, we demonstrate that RPA2 phosphorylation regulates the assembly of DNA damage-induced RPA and MRN foci. Using purified proteins, we observe a direct interaction between RPA with both NBS1 and MRE11. By utilizing RPA bound to ssDNA, we demonstrate that substituting RPA with phosphorylated RPA or a phosphomimetic weakens the interaction with the MRN complex. Also, the N-terminus of RPA1 is a critical component of the RPA−MRN protein−protein interaction. Deletion of the N-terminal oligonucleotide−oligosaccharide binding fold (OB-fold) of RPA1 abrogates interactions of RPA with MRN and individual proteins of the MRN complex. Further identification of residues critical for MRN binding in the N-terminus of RPA1 shows that substitution of Arg31 and Arg41 with alanines disrupts the RPA−MRN interaction and alters cell cycle progression in response to DNA damage. Thus, the N-terminus of RPA1 and phosphorylation of RPA2 regulate RPA−MRN interactions and are important in the response to DNA damage.

Replication protein A (RPA)[1] was originally purified as a replication factor that stimulated helicase strand displacement and polymerase synthesis (*1*). RPA is now known to be essential for many aspects of DNA metabolism, including initiating DNA damage checkpoint signaling and repair of DNA damage (*2*−*6*). RPA facilitates activities in replication and repair through its interactions with other proteins. Encountering a lesion that stalls the replication fork leads to the uncoupling of helicase and polymerase activities which generates long stretches of ssDNA that are stabilized by RPA binding (*7*, *8*). RPA recruits and interacts with ATRIP and ATR to facilitate the activation of ATR signaling (*9*). Following ATR recruitment, ATR phosphorylates RPA and a number of other substrates, including CHK1, MCM2, MCM7, RAD9, and RAD17, at the replication fork, presumably to stabilize the fork and promote the restart of replication (*10*).

Another protein complex involved in ATR and ATM signaling pathways is the MRN complex. This complex consists of MRE11, NBS1, and RAD50 and functions in DNA replication, DNA damage recognition, cell cycle checkpoint activation, and DNA repair (*11*). The MRN complex prevents double-strand breaks (DSBs) during replication in *Xenopus* extracts (*12*, *13*) and recruits ATM to DSBs through interaction with NBS1 (*14*, *15*). In addition, the nuclease activities of MRE11 facilitate UV-induced ATR signaling (*16*). In fact, RPA and the MRN complex colocalize to discrete foci and interact in response to DNA replication fork blockage induced by UV (*17*). It was recently shown that this protein−protein interaction involves an acidic α-helix peptide in MRE11 that binds to DNA binding domain (DBD) F located at the N-terminus of RPA1 (*18*). This RPA−MRN interaction was shown to be important for suppressing DNA replication initiation following DNA damage (*19*).

The functional role of RPA in DNA metabolism relies on DBDs that bind to ssDNA and disrupt duplex DNA structure (reviewed in ref *20*). These DBDs are OB folds that are present in each of the subunits of RPA, which includes RPA1 (p70), RPA2 (p32), and RPA3 (p14) subunits. RPA1 contains DBD A and B, which are responsible for RPA's high-affinity binding to ssDNA. DBD C is located in the C-terminus of RPA1, and DBD F is located in the N-terminus of RPA1. DBD D is in the central

[†]This study has been supported by research grants from the American Cancer Society (ACS, RSG-06-163-01-GMC) and the Ohio Cancer Research Associates, Inc., to S.M.P., National Institutes of Health Grant P20-RR018759, and the Department of Human and Health Services of Nebraska to G.O.

*To whom correspondence should be addressed: Department of Biochemistry and Cancer Biology, Mail Stop 1010, 3000 Arlington Ave., University of Toledo Health Science Campus, Toledo, OH 43614. Telephone: (419) 383-4152. Fax: (419) 383-6228. E-mail: Stephan.Patrick@utoledo.edu.

[1]Abbreviations: Ala-RPA2, mutant RPA2 with alanine substitutions at serine and threonine phosphorylation sites located within the segment of amino acids 1−33 of RPA2; Asp8-RPA2, mutant RPA2 with aspartic acid substitutions at serine and threonine phosphorylation sites located within the segment of amino acids 1−33 of RPA2; ATR, ataxia telangiectasia-related; ATRIP, ATR interacting protein; co-IPs, co-immunoprecipitations; DBD, DNA binding domain; DDR, DNA damage response; DSBs, double-strand breaks; ELISAs, enzyme-linked immunosorbent assays; HU, hydroxyurea; MRN, MRE11−RAD50−NBS1 complex; ΔN-RPA1, mutant RPA1 containing a deletion of amino acids 1−168; NER, nucleotide excision repair; OB, oligosaccharide/oligonucleotide binding; RPA, replication protein A; SA, streptavidin; SSB, single-strand DNA binding protein; ssDNA, single-stranded DNA; UV, ultraviolet.

Published on Web 07/08/2009

region of RPA2, and DBD E is within RPA3. The DBD F domain has a basic cleft region that has recently been suggested to control checkpoint protein−protein interactions (*21*, *22*). Multiple checkpoint proteins interact with the DBD F domain, including p53, ATRIP, RAD9, and MRE11 (*18*, *21*, *22*). The key to these protein interactions involves the basic cleft region of the DBD F domain binding to an acidic α helix domain located within the checkpoint proteins. Following DNA damage, RPA is hyperphosphorylated on the N-terminus of RPA2 (*23*). This phosphorylation has the potential to regulate RPA−protein interactions through the binding of the negatively charged N-terminus of RPA2 to the basic cleft region of DBD F. Indeed, when small peptides of the N-terminus of RPA2 were mutated via introduction of negatively charged amino acids designed to mimic phosphorylated residues, the acidic peptide interacted with the basic cleft of the DBD F domain (*21*, *24*).

Previously published results have shown that the RPA binding surface on MRE11 mapped to amino acids 521−569 and that an MRE11 peptide consisting of amino acids 539−553 bound to the N-terminus of RPA1 (*18*, *19*). In contrast to the previously published results, we directly compare wt-RPA1 and mutant RPA1 defective for MRN binding in cells with the complete MRN complex. In this manner, we more specifically implicate the N-terminus of RPA1 in the binding to the MRN complex. Additionally, we have determined that phosphorylation of RPA2 regulates RPA−MRN interactions and the assembly of RPA and NBS1 foci. Unlike the case in the previous publications, we identify an interaction between RPA and NBS1 using purified proteins. Our data and previous results suggest that the N-terminus of RPA1 interacts with the MRN complex in unperturbed cells and phosphorylation of RPA2 disrupts RPA−MRN interactions in response to DNA damage.

EXPERIMENTAL PROCEDURES

Materials. DNA oligonucleotides were purchased from IDT DNA Technologies (IDT), Inc. The RPA2 antibodies were purchased from Thermo Fisher Scientific and Bethyl Laboratories, and the V5 agarose immobilized and RPA1 antibodies were from Bethyl Laboratories. MRE11 and NBS1 antibodies were from Genetex Inc. and Bethyl Laboratories, and the RAD50 antibody was from Genetex Inc. The HA antibody was purchased from Covance, and the γ-H2AX antibody was purchased from Thermo Fisher Scientific. The Ultra TMB ELISA solution was from Pierce. The 96-well streptavidin plates were from Thermo Fisher Scientific. All other reagents and chemicals were from standard suppliers.

Cell Culture. All cells were maintained at 37 °C and 5% CO_2 in Dulbecco's modified Eagle's medium (Invitrogen) supplemented with 10% fetal bovine serum (Hyclone), 100 units/mL penicillin, and 100 μg/mL streptomycin. UMSCC38 cells are oral squamous cell carcinoma cells established at the University of Michigan (Ann Arbor, MI) and generously provided by T. Carey (University of Michigan). For etoposide treatment, cells were incubated in growth medium containing etoposide for 2 h and then replenished with fresh growth medium and incubated for 6 and 24 h after removal of etoposide.

Retroviral Gene Expression. Wild-type and alanine-substituted RPA32 cDNAs were inserted into retroviral vector pQCXIH (Clontech). RPA2 DNA sequences representing amino acids 18−271 were amplified from pET-11d vectors containing the wild-type and alanine-subsituted (RPA2, 4, 8, 11−13, 21, 23, 29, 33, and 39) RPA heterodimer (generously supplied by M. Wold, University of Iowa, Iowa City, IA) and were digested with BamHI and NaeI. Amino acids 1−17 were created by the ligation of two phosphorylated, double-stranded oligonucleotides with AgeI and NaeI overhangs. The N-terminal double-stranded oligonucleotides and the amplified C-terminus containing a HA tag sequence were ligated into AgeI/BamHI-digested pQCXIH. Wild-type and mutated RPA70 cDNAs were inserted into retroviral vector pQCXIP (Clontech). RPA70 was initially PCR amplified from the RPA-containing pET-11d vector using a NotI site-containing sense oligonucleotide and nested oligonucleotides encoding a C-terminal V5 tag containing an EcoRI site and ligated to cloning vector pGEM-t-easy (Promega). Truncated RPA70 (amino acids 1−167) was similarly created using an internal sense site. Aspartic acid to alanine substitutions at amino acids 31 and 41 were created by site-directed mutagenesis (New England Biolabs). Wild-type and mutated RPA70 were excised from pGEM-t-easy using restriction enzymes NotI and EcoRI and ligated into retroviral expression vector pQCXIP. For retroviral infection, Phoenix A cells were plated overnight in 60 mm culture dishes and transfected with plasmid using Lipofectamine 2000 (Invitrogen). After 48 h at 37 °C, cells were incubated for an additional 24 h at 32 °C. Supernatants were collected, centrifuged at 2000*g* for 10 min, and added to 25% confluent UMSCC38 cells in the presence of 10 μg/mL Polybrene (Sigma). After 48 h, UMSCC38 cells were selected with 40 μg/mL hygromycin or 500 ng/mL puromycin. Surviving cells were grown to near confluence and tested for expression of recombinant RPA by Western blot analysis.

Immunofluorescence. Cells were grown on 22 mm coverslips overnight prior to drug treatment. After an initial wash with PBS, cells were extracted with PBS containing 0.5% Triton X-100 for 5 min on ice and fixed with 4% paraformaldehyde for 15 min. Next, the coverslips were blocked with 15% FBS and then incubated with HA, NBS1, or γ-H2AX antibodies diluted in PBS containing 2% BSA overnight. The coverslips were then washed with PBS and incubated with Alexa Fluor 488-conjugated anti-mouse and Alexa Fluor 568-conjugated anti-rabbit antibodies for 1 h. Nuclei were stained with a 1 μg/mL 4′,6-diamidino-2-phenylindole solution. Immunofluorescent images were captured digitally with a Zeiss axiovert 200 M microscope.

Protein Purification. RPA and RPA mutants were purified as previously described using the expression vectors kindly provided by M. Wold (*25*). Hyperphosphorylated RPA was purified as previously described (*26*). Briefly, we purified hyperphosphorylated RPA by taking *Escherichia coli* extracts containing RPA and fractionating them on a ssDNA cellulose column. Bound RPA protein was eluted, and the resulting RPA fraction was approximately 80% pure. The RPA was dialyzed and mixed with HeLa extracts. The mixture was supplemented with an ATP regenerating system, ssDNA, and phosphatase inhibitors to inhibit phosphatase activity within the cell extracts. This reaction allows for endogenous kinases within the HeLa extract to phosphorylate RPA. Following incubation for 3 h at 30 °C, the hyperphosphorylated RPA was purified in a manner identical to that of recombinant RPA (*25*). MRN was purified using a procedure similar to that previously described (*27*). Briefly, 300 mL of Sf9 cells at a density of 1.25×10^6 cells/mL was infected with MRE11, RAD50, and NBS1 baculovirus (kindly provided by J. Carney). The MRE11 and NBS1 proteins contain a six-His tag. Cells were incubated for 48−72 h and harvested by centrifugation. Cells were dounce homogenized and sonicated followed

by centrifugation to remove cellular debris. The supernatant was loaded onto a 1 mL nickel column equilibrated in 10 mM imidazole. The gel matrix was washed with 10 mM imidazole followed by 20 and 30 mM imidazole washes. Bound MRN was eluted using 250 mM imidazole. In some instances, a mono Q column was also utilized to achieve greater purity (*27*). MRN and RPA purifications are shown in the Supporting Information as Figures S1 and S2, respectively.

Immunoprecipitations. For immunoprecipitation (IP) reactions with purified proteins, 300 or 500 ng of purified RPA and 2−4 μg of MRE11, NBS1 or partially purified MRN complex were allowed to interact at 4 °C for 30 min in PBS, 0.01% NP-40, and 1 mg of BSA. The proteins were then pulled down for 1 h with either 1 μg of specific antibody with Sepharose beads or Ni-NTA agarose beads. Reaction mixtures were washed with PBS with 0.01% NP-40 and analyzed by Western blotting. For the IPs using ssDNA, RPAs were preincubated with 42-mer ssDNA and then MRN protein was added and the mixture assessed as described above. For IPs with cell lysates, cells were washed with PBS and resuspended in cell lysis buffer [50 mM Tris-HCl (pH 7.5), 150 mM NaCl, 0.1% NP-40, 10 mM NaF, 10 mM β-glycerophosphate, 1 mM Na_3VO_4, and protease inhibitor cocktail] for 30 min on ice. Cell lysates were centrifuged for 20 min at 20000*g*. The supernatants were incubated with anti-V5 affinity gel (Sigma) at 4 °C overnight. The beads were washed three times with PBS containing 0.1% NP-40. The beads were resuspended in SDS sample buffer, boiled, and separated via SDS−PAGE.

Immunoblotting. Cell lysates and immunoprecipitates were separated by SDS−PAGE and transferred to polyvinylidene difluoride (PVDF) membranes. Membranes were immunoblotted using the following primary antibodies: RPA1, RPA2, MRE11, NBS1, and RAD50. Secondary antibodies were Alexa Fluor 680-conjugated anti-rabbit (Invitrogen) and DyLight 800-conjugated anti-mouse (ThermoFisher Scientific) antibodies. Blots were visualized using infrared fluorescence (LI-COR Inc.) or chemiluminescence.

ELISAs. For 2 h at 37 °C, 100 ng of protein was bound to the bottom of a 96-well plate and blocked for 1 h at 37 °C in PBS with 5% nonfat milk and 0.1% BSA, and then 2.5 pmol of purified RPA was added for 1 h. Next, the primary polyclonal RPA2 antibody (1:4000 dilution) was added followed by washing. The secondary goat anti-rabbit antibody (1:3000 dilution) was then added, and wells were washed. Finally, 100 μL of 1-Step Ultra TMB-ELISA solution was added, and the change in absorbance at 610 nm was monitored at 1 min intervals for 20 min and analyzed using SoftMax Pro (Molecular Devices Corp.). The relative binding activity is based on HRP activity that is determined as the change in absorbance at 610 nm/min. The reactions displayed linear kinetics for the duration of the assay (data not shown). For reactions with ssDNA, 2.5 pmol of RPA was incubated with 2.5 pmol of 42-mer ssDNA on ice before being added to the wells coated with 5 pmol of MRN, MRE11, or NBS1. For the streptavidin−biotin−ssDNA ELISA, 5 pmol of biotinylated ssDNA was added to the streptavidin-coated wells. RPAs were subsequently added and allowed to bind the biotinylated ssDNA. The wells were then washed to remove any inactive and unbound RPA and blocked with BSA and biotin before MRN was added to the wells. MRE11 primary and HRP-conjugated secondary antibodies were used for detection similar to that described above.

Chromatin Isolation. Chromatin fractionation was performed as previously described with slight modifications (*41*). Briefly, for the isolation of chromatin, the cells were washed once with PBS and incubated on ice in buffer A [10 mM HEPES (pH 7.9), 10 mM KCl, 1.5 mM $MgCl_2$, 0.34 M sucrose, 10% glycerol, 1 mM DTT, 10 mM NaF, 10 mM β-glycerophosphate, 1 mM Na_3VO_4, and phosphatase inhibitor cocktail] with 0.1% Triton X-100 for 5 min. Nuclei were collected by centrifugation (10 min at 1300*g* and 4 °C) and washed once with buffer A and lysed in buffer B [3 mM EDTA, 0.2 mM EGTA, 1 mM DTT, 10 mM NaF, 10 mM β-glycerophosphate, 1 mM Na_3VO_4, and phosphatase inhibitor cocktail (Calbiochem)] for 30 min on ice. Insoluble chromatin was collected by centrifugation (5 min at 1700*g* and 4 °C). The final chromatin pellet was resuspended in SDS sample buffer, boiled, and separated by SDS−PAGE.

RESULTS

Phosphorylation of RPA2 Regulates Colocalization of RPA and MRN Foci. At drug concentrations used in this study, most etoposide-stabilized cleavage complexes contain high levels of ssDNA breaks rather than dsDNA breaks (*28*−*30*). These ssDNA breaks can stall replication forks and if not stabilized lead to replication fork collapse and subsequent dsDNA breaks. The increased level of formation of RPA foci is consistent with the presence of etoposide-associated ssDNA breaks. NBS1 has been shown to associate with ssDNA lesions (*31*). It was previously reported that NBS1 and RPA do not colocalize immediately following etoposide treatment for 3 h (*32*). To determine whether the phosphorylation of RPA2 alters the assembly of RPA and MRN foci, we utilized UMSCC38 cells that express wt-RPA2 or Ala-RPA2 (Figure 1). Ala-RPA2 contains alanine substitutions at S4, S8, S11, S12, S13, T21, S23, S29, S33, and S39 within the N-terminus of RPA2 (Figure 1B). Endogenous RPA2 in both cell lines was down-regulated by stably expressing shRNA targeting the 3′-UTR of RPA2 (Figure 2A). Treatment with etoposide induced phosphorylation of RPA2 in the cells expressing wt-RPA2; however, no phosphorylation was detected in the cells expressing Ala-RPA2 (Figure 2B). DNA damage caused the assembly of NBS1 and RPA to intranuclear foci and phosphorylation of H2AX (Figure 2C,E). In the cells expressing wt-RPA2, NBS1 and RPA foci colocalized to a minor extent at 6 h which decreased by 24 h after etoposide treatment (Figure 2C, panels D−I, and Figure 2D). Cells expressing Ala-RPA2 contained RPA and MRN foci that colocalized at 6 h and continued to colocalize at 24 h (Figure 2C, panels M−R). Thus, while the phosphorylation of RPA2 is not required to recruit and assemble components of the MRN complex to sites of DNA damage, it does contribute to colocalization of MRN with RPA and the regulation of this process.

DBD-F of RPA Interacts with the MRN Complex, and Phosphorylation of RPA2 Weakens the Interaction. The persistent colocalization of the phospho mutant RPA with NBS1 suggested that the phosphorylation of wild-type RPA2 modulates the RPA−MRN interaction. Therefore, we initially utilized co-immunoprecipitations (co-IPs) and purified proteins to test whether phosphorylation of RPA2 alters the interaction of the protein with the MRN complex. We performed co-IPs with RPA bound to ssDNA, which more closely resembles RPA at DNA lesion sites (Figure 3A). In this experiment, we also utilized various mutant RPAs to identify the domains required for the

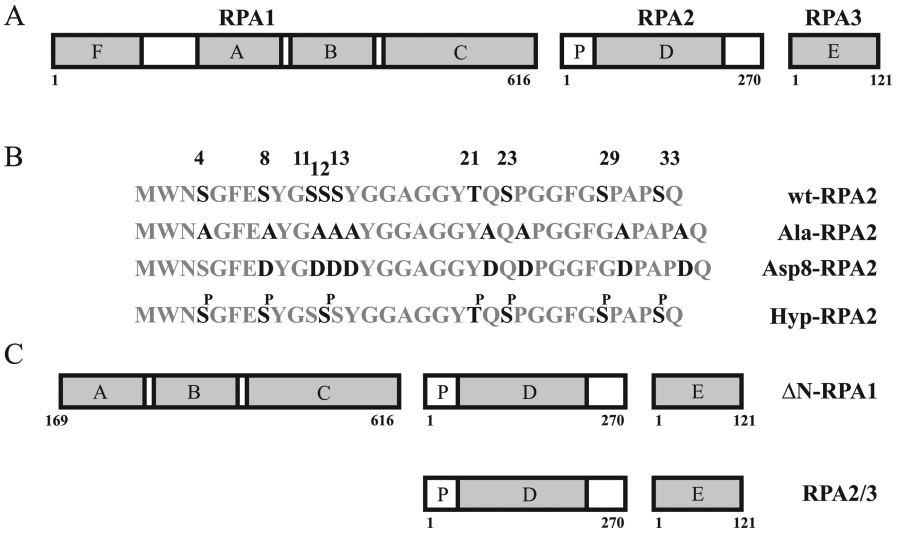

FIGURE 1: Diagram of RPA and RPA mutants used in this study. (A) Organization of the RPA heterotrimer. (B) Amino acid sequences of the RPA2 N-terminal domain used in this study, including wild-type RPA2 (wt-RPA2), alanine- and aspartic acid-substituted RPA2 (Ala-RPA2 and Asp8-RPA2, respectively), and the predicted residues affected by hyperphosphorylation (Hyp-RPA2). (C) RPA constructs containing either truncated (ΔN-RPA1) or omitted (RPA2/3) RPA1.

MRN interaction (Figure 1B,C). The Asp8-RPA2 mutant is a phosphomimetic that mimics hyperphosphorylated RPA containing aspartic acid substitutions at seven serines and one threonine within the segment of amino acids 1−40 of the N-terminus of RPA2, and ΔN-RPA1 has undergone a 1−168 N-terminal deletion of RPA1 (*24*, *33*). RPA2/3 consists of RPA2 and RPA3 and does not contain RPA1. We observed a 95% decrease in the level of interaction between the partially purified MRN complex and the RPA2/3 protein complex, indicating the primary interaction occurs with RPA1 (Figure 3A). When compared with the RPA−MRN interaction, Asp8-RPA2 and ΔN-RPA1 displayed 88 and 97% decreases, respectively, in their level of binding to the MRN complex when bound to ssDNA.

During the protein purification of RPA, a small amount of the protein becomes inactive, likely from the stringency of the chromatography conditions, and loses the ability to bind ssDNA. To eliminate the inactive pool of protein and account for possible differences in RPA and mutant RPA ssDNA binding activity in the co-IP experiments, we quantified the effects of RPA2 phosphorylation and the N-terminus of RPA1 on RPA−MRN interactions using ELISAs with streptavidin (SA)-bound plates and biotinylated ssDNA. In this assay, once active RPA and mutant RPA bind to ssDNA, the inactive protein forms are washed out of the wells. There is a decrease in the level of binding of Asp8-RPA2 to the MRN complex compared with RPA binding to MRN (Figure 3B, lane 2 compared with lane 1). Also, ΔN-RPA1 binds weakly to MRN when bound to ssDNA, and the relative absorbance is only just greater than the SSB and antibody controls (Figure 3B, lanes 3, 4, and 6, respectively). In the absence of RPA, we detect MRN binding to ssDNA (Figure 3B, lane 5). As a control, we used *E. coli* SSB to bind and block the MRN complex from binding ssDNA (Figure 3B, lane 4). Because of possible differences in RPA and mutant RPA ssDNA binding activities, the amount of active RPA proteins was determined for each protein and normalized to ensure equal amounts of RPA, Asp8-RPA2, and ΔN-RPA1 were bound to ssDNA (Figure 3C). The control reactions were performed using kinetic as well as end point analysis to ensure equal protein binding. These data support a role for the phosphorylation of RPA2 in modulating the RPA−MRN interaction when RPA is bound to ssDNA and also indicate that the N-terminus of RPA1 plays a critical role in the interaction with the MRN complex.

MRE11 and NBS1 Are Sufficient for RPA−MRN Interactions. We have previously demonstrated the ability to produce and purify biologically relevant hyperphosphorylated RPA by incubating partially purified recombinant RPA with a HeLa extract in the presence of phosphatase inhibitors. We identified the sites phosphorylated using mass spectrometry and phospho-specific antibodies and verified that the same RPA2 sites phosphorylated by HU- and UV-induced damage were phosphorylated with our HeLa extract method of phosphorylation (*26*). Having shown that RPA interacts with MRN, we wanted to further assess the interaction between RPA and components of the MRN complex. Here, we immunoprecipitated purified recombinant unphosphorylated and hyperphosphorylated RPA using an antibody directed against RPA2 to pull down the purified MRE11−NBS1 (MN) complex (Figure 4A). Both unphosphorylated RPA and hyperphosphorylated RPA interacted with MN; however, hyperphosphorylation of RPA2 weakened binding to MN by 70% (Figure 4A, RPA compared to Hyp-RPA).

RPA has previously been shown to interact with MRE11 (*17*). Our co-IP results with the MN complex suggest RPA has a higher binding affinity for NBS1 than MRE11. To further investigate the RPA−NBS1 interaction, we tested whether RPA binds directly to NBS1. We utilized nickel pull-downs (NBS1 is His-tagged) to assess the interaction of NBS1 with RPA. NBS1 was allowed to interact with RPA, and then proteins were bound to the nickel matrix. Using the nickel pull-down, RPA interacted with NBS1 (Figure 4B, lane 1). In contrast, RPA alone interacted minimally with the nickel matrix (Figure 4B, lane 2). To assess the effect of RPA phosphorylation on RPA−NBS1 interactions, binding of RPA and hyperphosphorylated RPA with NBS1 were examined. Purified RPA did interact with NBS1, and phosphorylation of RPA2 weakened this interaction 67% (Figure 4C). Overall, these data support an interaction between RPA and NBS1 and are consistent with our previous results that show phosphorylation of RPA2 weakens the interaction between RPA and the MRN complex.

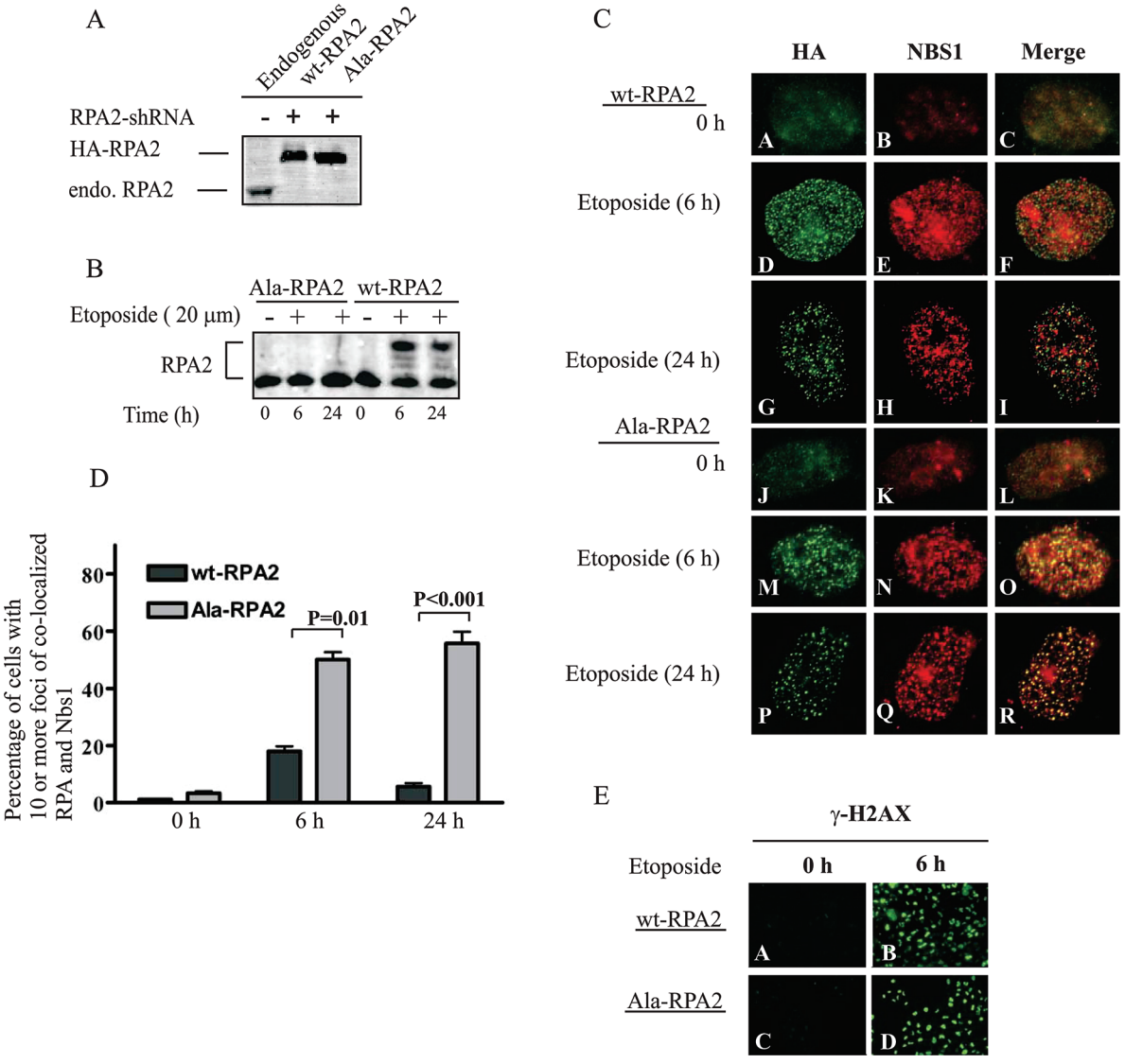

FIGURE 2: Phosphorylation of RPA2 restricts interactions between NBS1 and RPA. (A) Protein expression levels in UMSCC38 cells stably expressing HA-tagged wt-RPA2 and Ala-RPA2 and shRNA−RPA2 constructs were analyzed by separating cell lysates by SDS−PAGE and immunoblotting with a general anti-RPA2 antibody. (B, C, and E) UMSCC38 cells stably expressing wt-RPA2 or Ala-RPA2 with down-regulation of endogenous RPA2 were not treated (0 h) or were treated with etoposide (20 μM for 2 h) followed by recovery for 4 and 22 h. (B) Cell lysates were separated by SDS−PAGE and immunoblotted with RPA2 antibodies. (C) Fixed cells were stained with anti-HA and anti-NBS1 antibodies. (D) Cells were scored for RPA−MRN colocalization to DNA damage foci. Two hundred cells were scored per experiment. Error bars indicate standard errors (n = 3). P values were calculated using an unpaired, two-tailed t test. (E) Fixed cells were stained with anti-γ-H2AX antibodies.

RPA Bound to ssDNA Interacts with NBS1 and MRE11. RPA binds to both MRE11 and NBS1 in the absence of ssDNA, possibly at multiple OB binding surfaces on RPA. To determine whether ssDNA competes for these binding surfaces, we performed ELISAs using purified MRE11 and NBS1 with RPA and RPA mutants (Figure 5). We were unable to detect an interaction between RPA2/3 and NBS1 or MRE11 as indicated by the lack of signal above the Ab control (in Figure 5A,B, compare lanes 4 and lane 5). This indicates that the RPA1 subunit is critical for the interaction with both NBS1 and MRE11. Due to comparable properties for binding of Hyp-RPA2 and Asp8-RPA2 to the MRN complex and ssDNA, we used Asp8-RPA2 for the protein interactions with MRE11 and NBS1. For both NBS1 and MRE11, we observed a weakened interaction with Asp8-RPA2 and ΔN-RPA1 compared with RPA in the presence of ssDNA (Figure 5A,B, lanes 1−3) consistent with the RPA−MRN binding results. These data support a role for RPA−NBS1 and RPA−MRE11 interactions when RPA is bound to ssDNA.

Interaction of MRN with RPA Requires the Basic Cleft of the N-Terminus of RPA1. The N-Terminus of RPA70 Is Important in the Cellular Response to DNA Damage. Our data indicate the N-terminus of RPA1 is necessary for binding to the MRN complex when RPA is bound to ssDNA. Therefore, we hypothesized that mutating basic residues in the cleft of the N-terminal domain would disrupt the interaction between RPA and the MRN complex. To test this hypothesis, an RPA1 mutant was generated with alanine substitutions for residues Arg31 and Arg41 which are located in the basic cleft of the N-terminal domain. V5-wt-RPA1 and V5-Ala31/Ala41-RPA1 were expressed in UMSCC38 cells. Immunoprecipitation of V5-wt-RPA1 protein complexes from chromatin fractions indicated they contained endogenous NBS1 (Figure 6A, lanes 2 and 3). After etoposide treatment, the wild-type form of RPA1 was

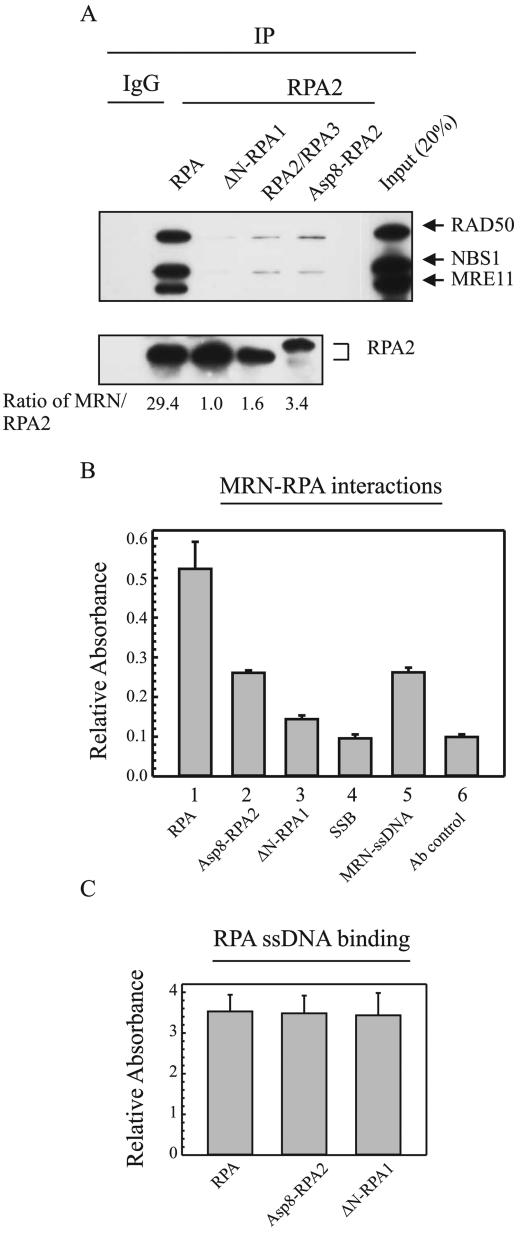

FIGURE 3: Interaction of RPA with the MRN complex requires the N-terminus of RPA1 and is regulated by RPA2 phosphorylation. (A) Various purified RPAs were used to assess the protein−protein interactions. RPAs (2.5 pmol) were incubated with ssDNA (5 pmol) prior to the addition of the MRN (5 pmol) complex expressed and purified from baculovirus preparations. RPA2 antibodies were used to immunoprecipitate wt-RPA and the RPA mutants. The MRN and RPA2 levels were quantitated with NIH image. The numbers are the ratios of MRN to RPA2 normalized to the ratio for the ΔNRPA1 sample. Abbreviations: RPA, wt-RPA; ΔN-RPA1, N-terminal deletion of RPA1 (1−168); RPA2/RPA3, RPA without RPA1; Asp8-RPA2, a phosphomimetic of RPA2. (B and C) Biotin-labeled ssDNA bound to streptavidin-coated 96-well plates was incubated with wild-type and mutant RPAs. (B) The wild type, Asp8-RPA2, and ΔN-RPA1 were added to wells coated with biotin-labeled ssDNA bound to streptavidin. The wells were washed to remove unbound RPA and blocked with BSA and biotin. Purified MRN (5 pmol) was subsequently added to the wells, and protein interactions were detected using MRE11 and HRP-conjugated antibodies. The SSB control represents the *E. coli* single-strand binding protein coating the biotin-labeled DNA prior to addition of MRN, and the MRN−ssDNA sample represents MRN binding without prior RPA addition. (C) The amount of purified RPA (2.5−3.0 pmol) bound to ssDNA was detected with RPA2 and HRP-conjugated antibodies and normalized on the basis of the absorbance at 610 nm.

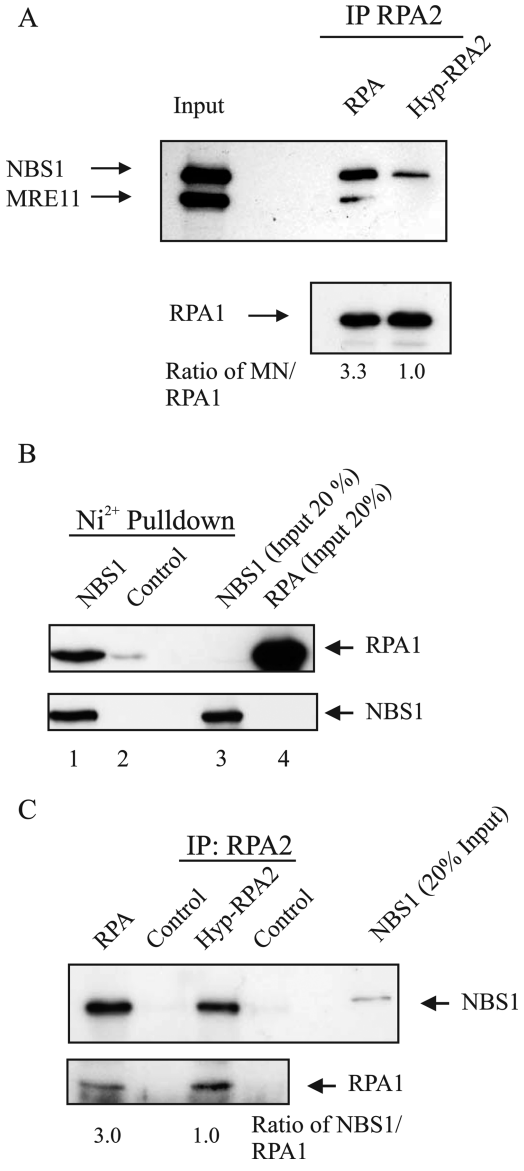

FIGURE 4: RPA binds to the MRE11−NBS1 complex and to NBS1. (A) Purified RPA and hyperphosphorylated RPA (Hyp-RPA) (2.5 pmol) were incubated with the MRE11−NBS1 complex (5 pmol) followed by addition of RPA2 antibodies and protein G−agarose beads. Proteins bound to the beads were eluted and separated by SDS−PAGE and immunoblotted with RPA1, NBS1, and MRE11 antibodies. The numbers are the ratios of MN to RPA1 and normalized to the ratio for the Hyp-RPA sample. (B) His-NBS1 (5 pmol) was incubated with RPA (2.5 pmol) and then pulled down with Ni^{2+} matrix. Proteins bound to the beads were eluted and separated by SDS−PAGE and immunoblotted with RPA1 and NBS1 antibodies. (C) Purified RPA (2.5 pmol) and Hyp-RPA (2.5 pmol) were incubated with purified NBS1 (5 pmol). Immunoprecipitated proteins were separated by SDS−PAGE followed by immunoblotting with NBS1 and RPA1 antibodies. The numbers are the ratios of NBS1 to RPA1 and normalized to the ratio for the Hyp-RPA sample.

immunoprecipitated from chromatin while the mutant form associated with chromatin only after etoposide treatment (Figure 6A, lanes 3 and 5). The increase in the amount of V5-wt-RPA1 immunoprecipitated from chromatin was not accompanied by an increased amount of endogenous NBS1 associated with V5-wt-RPA1 (Figure 6A, lane 3). It is worth noting that these IP reactions were performed immediately after the 2 h etoposide incubation without any recovery time. In contrast to V5-wt-RPA1, immunoprecipitated V5-Ala31/Ala41-RPA1 from

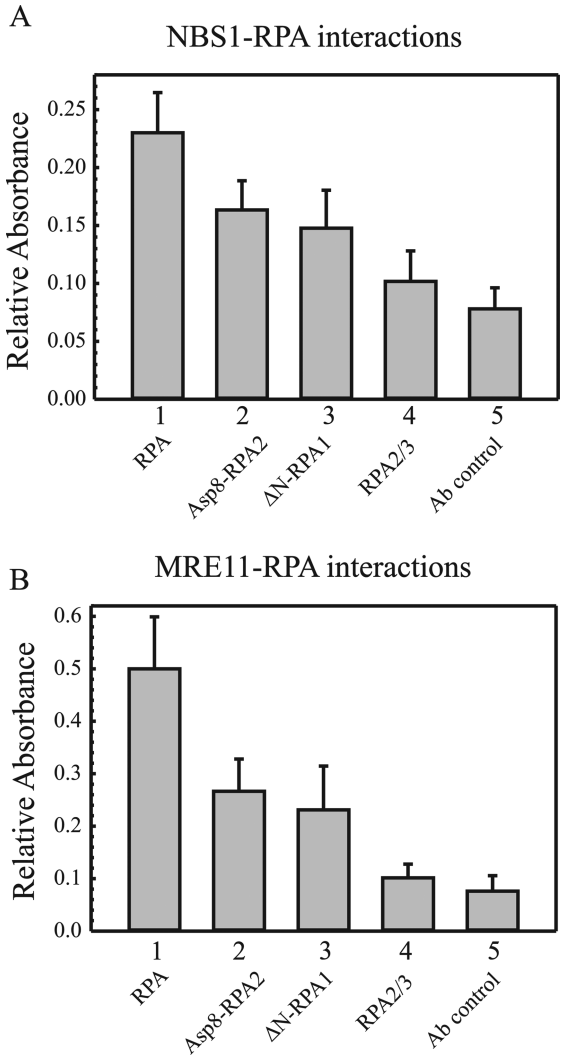

FIGURE 5: RPA interacts with both MRE11 and NBS1. (A and B) A modified ELISA was performed as described in Materials and Methods. Purified RPA, Asp8-RPA2, ΔN-RPA1, and RPA2/3 (2.5 pmol) were preincubated with ssDNA (2.5 pmol) before addition to the 96-well plates coated with purified (A) NBS1 or (B) MRE11 (5 pmol/well). Primary antibodies directed against RPA2 were added followed by the addition of HRP-conjugated secondary antibodies. The absorbance at 610 nm was measured over a period of 20 min. The relative absorbance values represent the affinities of the RPA forms for NBS1 and MRE11.

etoposide-treated cells did not contain detectable endogenous NBS1 (Figure 6A, lane 5). These results confirm that the conserved basic cleft in the N-terminus of RPA1 is required for stable RPA−MRN interactions.

To test the importance of the N-terminus of RPA1 in the DDR, cells were treated with 50 μM etoposide for 2 h and the drug was washed out. RPA1 siRNA effectively downregulated endogenous RPA1 without affecting the resistant exogenous form (Figure 6B). Progression through the cell cycle was detected by propidium iodide staining of DNA content and analyzed by flow cytometry. The cells expressing V5-wt-RPA1 arrested at G2 phase by 24 h, consistent with the parent UMSCC38 cells. In contrast, the V5-Ala31/Ala41-RPA1 mutants accumulated more in the S phase and less in the G2 phase (Figure 6C,D). These data provide evidence that the N-terminal domain of RPA1 functions by interacting with multiple proteins, including the MRN complex, in the cellular response to replication stress.

DISCUSSION

When cells are treated with such diverse agents as etoposide, cisplatin, or UV, it has been assumed that the unique DNA adducts that form are responsible for the activation of the DDR pathway. However, recent work has suggested that these DNA adducts are converted into a common structure that involves uncoupling of the replication helicase and polymerases, generating long stretches of ssDNA (*8*, *34*−*36*). Consistent with this idea, a primed ssDNA substrate with 5′- and 3′-junctions and ssDNA gaps mimicked a stalled replication fork and activated ATR checkpoint signaling in *Xenopus* extracts (*37*). A single free 5′-junction on a primed template was shown to induce ATR-dependent phosphorylation of Chk1 and Rad1 in *Xenopus* extracts (*37*). This is of interest because RPA binds ssDNA with a defined polarity (*38*, *39*). The orientation of an RPA trimer is in a 5′−3′ direction with the N-terminus of RPA1 at the 5′-end and the C-terminus of RPA1 as well as RPA2 at the 3′-end. This would place the N-terminus of RPA1 at the 5′-double-stranded−single-stranded junction. Many important proteins bind to the N-terminus of RPA1, including Rad9, part of the DNA damage-activated Rad9-Hus1-Rad1 clamp, and the ATR interacting partner, ATRIP (*18*, *22*). A recent analysis showed that cells expressing an RPA1 R41E/R43E mutant caused a defect in CHK1 phosphorylation following UV radiation (*18*). Consistent with this analysis, our data show cells expressing the RPA1 basic cleft mutant, A31A41-RPA1, do not accumulate exclusively in G2/M phase following etoposide treatment.

The N-terminus of RPA1 is attached to the rest of RPA1 through a flexible linker (*40*). This flexibility may be important to allow RPA to recruit different DNA damage response proteins, and the DNA binding polarity of RPA would ensure these proteins are directed to the lesion site for further activation of the DDR. Moreover, our data suggest that proteins that bind to the N-terminus of RPA1 are potentially assembled or disassembled from protein complexes by DNA damage-induced phosphorylation of RPA2; this implicates both the N-terminus of RPA1 and RPA2 in directing and controlling protein interactions at the site of the lesion. If the N-terminus of RPA1 binds ssDNA and also functions as a protein interaction domain, what role would RPA2 phosphorylation have in modulating these functions? One intriguing possibility is that the phosphorylation of RPA2 competes with proteins bound to RPA1, thus displacing them from RPA1. This is consistent with the interaction that was observed between a phosphomimetic RPA2 and the N-terminus of RPA1 (*21*, *24*). For example, our data demonstrate that the N-terminus of RPA1 is required for NBS1 and MRE11 binding and phosphorylation of RPA2 weakens these protein interactions. We propose that before RPA2 is phosphorylated, RPA interacts with NBS1 and MRE11 during unperturbed DNA replication and then, following DNA damage-induced phosphorylation of RPA2, RPA2 displaces NBS1 and MRE11 from RPA1. This would allow the MRN complex to act with additional factors to assist in stabilization of the lesion or relocate to other sites in the genome. In *Xenopus laevis* egg extracts, the MRN complex relocates to restarting replication forks to promote recovery of replication following DNA damage (*13*). In summary, our data suggest that the molecular lever-like action of RPA2 interacting with the N-terminus of RPA1 allows RPA to orchestrate multiple interactions at sites of DNA damage in a dynamic process that stabilizes the site of the lesion and assists in its repair.

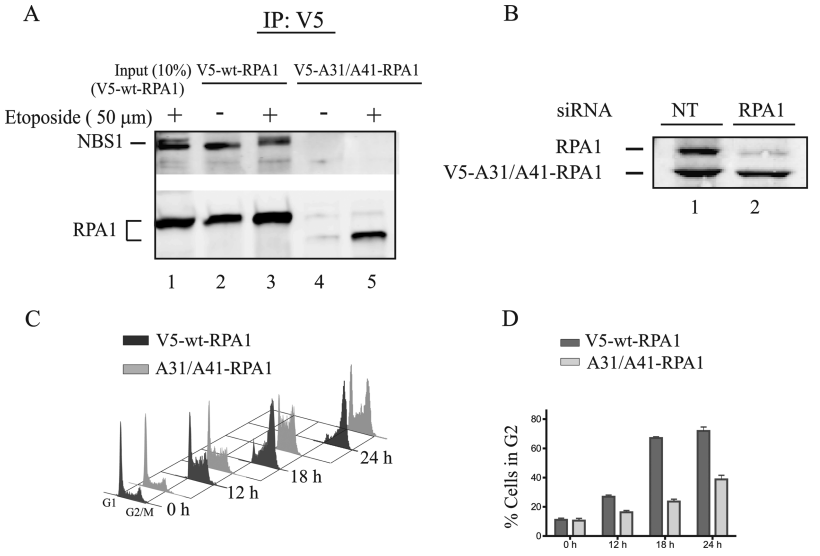

FIGURE 6: Basic cleft of the N-terminal domain of RPA1 that is required for RPA−MRN interaction. Cells stably expressing V5-RPA1 or V5-Ala31/Ala41-RPA1 were not treated or were treated with etoposide (50 μM for 2 h). Chromatin lysates were prepared and incubated with anti-V5 agarose beads. In panel A, the immunoprecipitated proteins were separated by SDS−PAGE, followed by immunoblotting with antibodies to NBS1 and RPA1. (B) Cells were treated with the RPA1−siRNA complex or nontargeting siRNA (NT) for 48 h. Cell lysates were separated by SDS−PAGE and immunoblotted with RPA1 antibodies. (C) UMSCC38 cells and cells expressing V5-wt- and V5-Ala31/Ala41-RPA1 were treated with the RPA1−siRNA complex or nontargeting siRNA (NT) for 48 h. Cells were then exposed to 50 μM etoposide for 2 h or not treated (0 h) followed by recovery for 10, 16, and 22 h. DNA content was measured by flow cytometry. The results are representative of two independent experiments. In panel D, the quantification of the percent of cells in G2 is presented.

ACKNOWLEDGMENT

We thank Anbarasi Kothandapani, Sanjeevani Arora, and Venkata Srinivas Mohan Nimai Dangeti for critical reading of the manuscript.

SUPPORTING INFORMATION AVAILABLE

Purification of MRN and RPA (Figures S1 and S2, respectively). This material is available free of charge via the Internet at http://pubs.acs.org.

REFERENCES

1. Wobbe, C. R., Weissbach, L., Borowiec, J. A., Dean, F. B., Murakami, Y., Bullock, P., and Hurwitz, J. (1987) Replication of simian virus 40 origin-containing DNA in vitro with purified proteins. *Proc. Natl. Acad. Sci. U.S.A. 84*, 1834–1838.
2. Ramilo, C., Gu, L., Guo, S., Zhang, X., Patrick, S. M., Turchi, J. J., and Li, G. M. (2002) Partial reconstitution of human DNA mismatch repair in vitro: Characterization of the role of human replication protein A. *Mol. Cell. Biol. 22*, 2037–2046.
3. Park, M. S., Ludwig, D. L., Stigger, E., and Lee, S. H. (1996) Physical interaction between human RAD52 and RPA is required for homologous recombination in mammalian cells. *J. Biol. Chem. 271*, 18996–19000.
4. Golub, E. I., Gupta, R. C., Haaf, T., Wold, M. S., and Radding, C. M. (1998) Interaction of human rad51 recombination protein with single-stranded DNA binding protein, RPA. *Nucleic Acids Res. 26*, 5388–5393.
5. Perrault, R., Cheong, N., Wang, H., Wang, H., and Iliakis, G. (2001) RPA facilitates rejoining of DNA double-strand breaks in an in vitro assay utilizing genomic DNA as substrate. *Int. J. Radiat. Biol. 77*, 593–607.
6. Aboussekhra, A., Biggerstaff, M., Shivji, M. K., Vilpo, J. A., Moncollin, V., Podust, V. N., Protic, M., Hubscher, U., Egly, J. M., and Wood, R. D. (1995) Mammalian DNA nucleotide excision repair reconstituted with purified protein components. *Cell 80*, 859–868.
7. Michael, W. M., Ott, R., Fanning, E., and Newport, J. (2000) Activation of the DNA replication checkpoint through RNA synthesis by primase. *Science 289*, 2133–2137.
8. Byun, T. S., Pacek, M., Yee, M. C., Walter, J. C., and Cimprich, K. A. (2005) Functional uncoupling of MCM helicase and DNA polymerase activities activates the ATR-dependent checkpoint. *Genes Dev. 19*, 1040–1052.
9. Zou, L., and Elledge, S. J. (2003) Sensing DNA damage through ATRIP recognition of RPA-ssDNA complexes. *Science 300*, 1542–1548.
10. Cimprich, K. A., and Cortez, D. (2008) ATR: An essential regulator of genome integrity. *Nat. Rev. Mol. Cell Biol. 9*, 616–627.
11. Lavin, M. F. (2007) ATM and the Mre11 complex combine to recognize and signal DNA double-strand breaks. *Oncogene 26*, 7749–7758.
12. Costanzo, V., Robertson, K., Bibikova, M., Kim, E., Grieco, D., Gottesman, M., Carroll, D., and Gautier, J. (2001) Mre11 protein complex prevents double-strand break accumulation during chromosomal DNA replication. *Mol. Cell 8*, 137–147.
13. Trenz, K., Smith, E., Smith, S., and Costanzo, V. (2006) ATM and ATR promote Mre11 dependent restart of collapsed replication forks and prevent accumulation of DNA breaks. *EMBO J. 25*, 1764–1774.
14. Falck, J., Coates, J., and Jackson, S. P. (2005) Conserved modes of recruitment of ATM, ATR and DNA-PKcs to sites of DNA damage. *Nature 434*, 605–611.
15. You, Z., Chahwan, C., Bailis, J., Hunter, T., and Russell, P. (2005) ATM Activation and Its Recruitment to Damaged DNA Require Binding to the C Terminus of Nbs1. *Mol. Cell. Biol. 25*, 5363–5379.
16. Buis, J., Wu, Y., Deng, Y., Leddon, J., Westfield, G., Eckersdorff, M., Sekiguchi, J. M., Chang, S., and Ferguson, D. O. (2008) Mre11 Nuclease Activity Has Essential Roles in DNA Repair and Genomic Stability Distinct from ATM Activation. *Cell 135*, 85–96.
17. Robison, J. G., Elliott, J., Dixon, K., and Oakley, G. G. (2004) Replication protein A and the Mre11·Rad50·Nbs1 complex co-localize and interact at sites of stalled replication forks. *J. Biol. Chem. 279*, 34802–34810.
18. Xu, X., Vaithiyalingam, S., Glick, G. G., Mordes, D. A., Chazin, W. J., and Cortez, D. (2008) The basic cleft of RPA70N binds multiple checkpoint proteins, including RAD9, to regulate ATR signaling. *Mol. Cell. Biol. 28*, 7345–7353.
19. Olson, E., Nievera, C. J., Liu, E., Lee, A. Y., Chen, L., and Wu, X. (2007) The Mre11 complex mediates the S-phase checkpoint through an interaction with replication protein A. *Mol. Cell. Biol. 27*, 6053–6067.
20. Wold, M. S. (1997) Replication protein A: A heterotrimeric, single-stranded DNA-binding protein required for eukaryotic DNA metabolism. *Annu. Rev. Biochem. 66*, 61–92.
21. Bochkareva, E., Kaustov, L., Ayed, A., Yi, G. S., Lu, Y., Pineda-Lucena, A., Liao, J. C., Okorokov, A. L., Milner, J., Arrowsmith, C. H., and Bochkarev, A. (2005) Single-stranded DNA mimicry in the

p53 transactivation domain interaction with replication protein A. *Proc. Natl. Acad. Sci. U.S.A. 102*, 15412–15417.
22. Ball, H. L., Ehrhardt, M. R., Mordes, D. A., Glick, G. G., Chazin, W. J., and Cortez, D. (2007) Function of a conserved checkpoint recruitment domain in ATRIP proteins. *Mol. Cell. Biol. 27*, 3367–3377.
23. Binz, S. K., Sheehan, A. M., and Wold, M. S. (2004) Replication protein A phosphorylation and the cellular response to DNA damage. *DNA Repair 3*, 1015–1024.
24. Binz, S. K., Lao, Y., Lowry, D. F., and Wold, M. S. (2003) The phosphorylation domain of the 32-kDa subunit of replication protein A (RPA) modulates RPA-DNA interactions. Evidence for an intersubunit interaction. *J. Biol. Chem. 278*, 35584–35591.
25. Henricksen, L. A., Umbricht, C. B., and Wold, M. S. (1994) Recombinant replication protein A: Expression, complex formation, and functional characterization. *J. Biol. Chem. 269*, 11121–11132 [erratum, (1994) *J. Biol. Chem. 269*, 16519].
26. Patrick, S. M., Oakley, G. G., Dixon, K., and Turchi, J. J. (2005) DNA damage induced hyperphosphorylation of replication protein A. 2. Characterization of DNA binding activity, protein interactions, and activity in DNA replication and repair. *Biochemistry 44*, 8438–8448.
27. Lee, J. H., and Paull, T. T. (2006) Purification and biochemical characterization of ataxia-telangiectasia mutated and Mre11/Rad50/Nbs1. *Methods Enzymol. 408*, 529–539.
28. Wozniak, A. J., and Ross, W. E. (1983) DNA damage as a basis for 4'-demethylepipodophyllotoxin-9-(4,6-O-ethylidene-β-D-glucopyranoside) (etoposide) cytotoxicity. *Cancer Res. 43*, 120–124.
29. Bromberg, K. D., Burgin, A. B., and Osheroff, N. (2003) A two-drug model for etoposide action against human topoisomerase IIα. *J. Biol. Chem. 278*, 7406–7412.
30. Long, B. H., Musial, S. T., and Brattain, M. G. (1985) Single- and double-strand DNA breakage and repair in human lung adenocarcinoma cells exposed to etoposide and teniposide. *Cancer Res. 45*, 3106–3112.
31. Bekker-Jensen, S., Lukas, C., Kitagawa, R., Melander, F., Kastan, M. B., Bartek, J., and Lukas, J. (2006) Spatial organization of the mammalian genome surveillance machinery in response to DNA strand breaks. *J. Cell Biol. 173*, 195–206.
32. Robison, J. G., Lu, L., Dixon, K., and Bissler, J. J. (2005) DNA lesion-specific co-localization of the Mre11/Rad50/Nbs1 (MRN) complex and replication protein A (RPA) to repair foci. *J. Biol. Chem. 280*, 12927–12934.
33. Gomes, X. V., and Wold, M. S. (1996) Functional domains of the 70-kilodalton subunit of human replication protein A. *Biochemistry 35*, 10558–10568.
34. Lopes, M., Foiani, M., and Sogo, J. M. (2006) Multiple mechanisms control chromosome integrity after replication fork uncoupling and restart at irreparable UV lesions. *Mol. Cell 21*, 15–27.
35. Stokes, M. P., Van Hatten, R., Lindsay, H. D., and Michael, W. M. (2002) DNA replication is required for the checkpoint response to damaged DNA in *Xenopus* egg extracts. *J. Cell Biol. 158*, 863–872.
36. Walter, J., and Newport, J. (2000) Initiation of eukaryotic DNA replication: Origin unwinding and sequential chromatin association of Cdc45, RPA, and DNA polymerase α. *Mol. Cell 5*, 617–627.
37. MacDougall, C. A., Byun, T. S., Van, C., Yee, M. C., and Cimprich, K. A. (2007) The structural determinants of checkpoint activation. *Genes Dev. 21*, 898–903.
38. Bochkarev, A., Pfuetzner, R. A., Edwards, A. M., and Frappier, L. (1997) Structure of the single-stranded-DNA-binding domain of replication protein A bound to DNA. *Nature 385*, 176–181.
39. de Laat, W. L., Appeldoorn, E., Sugasawa, K., Weterings, E., Jaspers, N. G., and Hoeijmakers, J. H. (1998) DNA-binding polarity of human replication protein A positions nucleases in nucleotide excision repair. *Genes Dev. 12*, 2598–2609.
40. Jacobs, D. M., Lipton, A. S., Isern, N. G., Daughdrill, G. W., Lowry, D. F., Gomes, X., and Wold, M. S. (1999) Human replication protein A: Global fold of the N-terminal RPA-70 domain reveals a basic cleft and flexible C-terminal linker. *J. Biomol. NMR 14*, 321–331.
41. Méndez, J., and Stillman, B. (2000) Chromatin Association of Human Origin Recognition Complex, Cdc6, and Minichromosome Maintenance Proteins during the Cell Cycle: Assembly of Prereplication Complexes in Late Mitosis. *Mol. Cell. Biol. 20*, 8602–8612.